LINEAR THEORY OF COUPLING EM POWER FROM WAVEGUIDE ARRAYS TO A PLASMA IN A MAGNETIC FIELD

A. Bers and K.S. Theilhaber

PFC/JA-81-20 November 1981

Linear Theory of Coupling EM Power From Waveguide Arrays to a Plasma in a Magnetic Field *

A. Bers and K. S. Theilhaber

Plasma Fusion Center
Massachusetts Institute of Technology
Cambridge, Massachusetts 02139

Abstract

A general, linear theory of coupling electromagnetic fields from free-space waveguides to an inhomogeneous plasma in a magnetic field is presented. Full account is taken of all the waveguide modes and the complete electrodynamics of the cold, inhomogeneous plasma in the coupling region. Far away from the coupling region the plasma is assumed to be absorptive (or to have a known reflectivity) and the waveguides to propagate only their dominant modes. The formulation is geared to obtain the reflection coefficients in the waveguides and the excitation of waves in the plasma. The results are applicable to RF heating of plasmas whose size is large compared to the waveguide array, as would be the case in a fusion reactor, and valid for the frequency regimes of either ion-cyclotron (harmonic), or lower-hybrid, or electron-cyclotron (harmonic) heating.

* Work supported by DOE Contract DE-AC02-78ET-51013 and NSF Grant No. ENG 79-07047.

I. Introduction

In what is generically known as "RF heating" and current generation of plasmas, electromagnetic (EM) energy from high-power sources external to the plasma is used to excite electromagnetic fields that propagate into the plasma and eventually dissipate their energy and momentum on the charged particles of the plasma, thus achieving the desired heating and/or current generation. One important aspect of such interactions is the coupling of power from the EM sources in free-space to the EM fields in the plasma. In magnetically confined plasmas with appreciable bulk temperatures, which are of interest in achieving fusion temperatures in a quasi steady-state, coupling structures cannot be inserted into the plasma and such coupling must take place at the plasma edge. Under these circumstances, and for technological reasons which we will not go into here, it is useful to consider EM sources at high frequencies whose energy can be brought conveniently to the plasma edge by waveguides. Specific heating and current generation schemes require that the excited fields have a prescribed spatial spectrum. This then requires that the waveguides be fed with specific relative amplitudes and phases, thus forming waveguide arrays.

In this paper we formulate a general linear theory to describe the coupling of EM power from waveguides to a plasma in a magnetic field. The coupling region (see Fig. 1) is taken as the inhomogeneous plasma extending from the free-space waveguide openings in the plasma wall to where the desired plasma modes are excited. The excited plasma modes are assumed to be dissipated beyond the coupling region, further into the plasma core. The plasma is taken to be of sufficiently large (reactor) size so that the limited extent of the coupling region can be modeled in slab geometry. (See Figs. 2 and 3.) For definiteness, the plasma in the coupling region is described by the cold plasma model with inhomogeneous density and magnetic field in one direction, into the plasma. This can be readily extended to include corrections due to finite temperatures and their variations, as needed. The walls of the plasma and waveguides are assumed perfectly conducting, and *the waveguides are allowed to be of arbitrary cross section*; the medium in the waveguides is taken as free-space. Far from the plasma wall the waveguides are assumed to propagate only their dominant mode. Given the amplitudes and phases of the incident fields in each of the waveguides and the unperturbed characteristics of the plasma in the coupling region, we show how to determine the reflection coefficient in each of the waveguides and the excited fields and power flow into the plasma modes in and beyond the coupling region.

The plasma modes amenable to waveguide excitation for heating a reactor type plasma fall

into three frequency ranges: (a) ion-cyclotron range of frequencies (ICRF), from the ion-cyclotron frquency ($\Omega_i/2\pi$) to a few times ($\Omega_i/2\pi$); (b) lower-hybrid range of frequencies (LHRF) which is around the ion plasma frequency ($\omega_{pi}/2\pi$); (c) electron cyclotron range of frequencies (ECRF) from the electron cyclotron frequency ($\Omega_e/2\pi$) to a few times ($\Omega_e/2\pi$). For magnetically confined fusion plasmas, in externally applied magnetic fields in the range of 5-10 Tesla, the ICRF would involve waveguides whose cross sectional dimensions would be comparable to a reactor plasma radius; for plasma densities in the range of $10^{20} - 10^{21}/m^3$ the LHRF fall in the usual microwave regime and the waveguide dimensions become smaller than a reactor plasma radius; finally, in the ECRF the waveguides are much smaller than the plasma radius. In all cases, the finite size of all the cross sectional dimensions of the waveguide relative to the plasma dimensions must be accounted for in the coupling problem.

Previous analyses of the waveguide-plasma coupling problem have concentrated on the LHRF [1,2,3,4]. All of these analyses were carried out in detail in only two dimensions: the waveguides were assumed to be perfectly conducting parallel-plates of infinite extent in the direction perpendicular to the confining magnetic field $\overline{B}_o$, and the excited plasma modes were thus forced to have no variation in that direction. These analyses were also concerned mainly with the dominant mode in the waveguides and neglected all of the higher-order modes that are required for a proper description of the fields at the plasma wall where the waveguide ends. In the present analysis these restrictions are removed; full account is taken of the finite dimensions of the waveguides in both the direction along $\overline{B}_o$ and the direction perpendicular to $\overline{B}_o$, and all the higher-order waveguide modes are accounted for in the vicinity of the waveguide opening in the plasma wall. In addition, we do not restrict ourselves to any particular frequency regime. Instead, the differential equations describing the fields in the inhomogeneous plasma, in the coupling region, are derived to apply to any of the frequency regimes. In general, these are four coupled first-order differential equations with nonconstant coefficients, and without further approximations their solutions must be arrived at by numerical techniques. Such numerical integrations are not carried out in this paper, but as a guide to work in the future several approximate solutions are outlined in an appendix. This together with the mode expansion for the fields in the waveguides is shown to lead to a complete solution of the linear coupling problem.

Section II describes the mode expansion of the waveguide fields. Section III describes the plasma fields and their Fourier transforms in the two directions of assumed plasma homogeneity. Section IV gives the solution of the coupling problem from a single waveguide. Section V general-

izes the solution of the coupling problem to multiple waveguides (waveguide arrays) independently fed in amplitude and phase. Section VI summarizes the results and discusses the limitations of the assumed model and analysis. The detailed description of the waveguide mode formalism used in the paper is given in Appendix A, and the differential equations for the plasma fields in the coupling region, as well as some of their approximate solutions, are derived in Appendix B.

II. The Waveguide Fields

We consider an arbitrary cylindrical waveguide, i.e. one which is uniform in the x-direction and of arbitrary cross section transverse to x. Figure 2 illustrates a waveguide of rectangular cross section, but our description is equally applicable to any other cross section, e.g. circular or elliptical. For simplicity we shall assume that the waveguide walls are perfectly conducting, and that the plasma does not penetrate into the waveguide so that the medium enclosed by the waveguide walls is taken as free-space (ϵ_0, μ_0). The solution of Maxwell's equations in such cylindrical waveguides is well known [5]. The electromagnetic fields can be expressed as the superposition of an infinite set of orthogonal E (or TM) modes and H (or TE) modes which are complete. A summary of these modes, in a conveniently normalized form, is given in Appendix A. For our purposes, we assume that at the frequency of interest the waveguide propagates only its dominant (lowest-order) mode, and all other (higher-order) modes are below cutoff. The transverse fields in the waveguide can then be written as follows:

$$\overline{E}_T^w = \frac{V_{+0}}{1+R}\left(e^{ik_d x} + R\,e^{-ik_d x}\right)\bar{e}_d(y,z) + \sum_H V_{-H}\,e^{\alpha_H x}\,\bar{e}_H(y,z) \tag{1}$$

$$\overline{H}_T^w = \frac{Y_d^w V_{+0}}{1+R}\left(e^{ik_d x} - R\,e^{-ik_d x}\right)\bar{h}_d(y,z) + \sum_H -Y_H^w V_{-H}\,e^{\alpha_H x}\,\bar{h}_H(y,z)\,. \tag{2}$$

The dominant mode is characterized by (see Appendix A) wavenumber $k_d = (2\pi/\lambda_g)$, normalized transverse field patterns $\bar{e}_d$ and $\bar{h}_d$, waveguide admittance Y_d^w , incident field amplitude V_{+0} (referenced to $x = 0$, or any place an integer multiple of $\lambda_g/2$ to the left of $x = 0$), and complex reflection coefficient R. The higher-order modes are all evanescent from $x = 0$ toward $x < 0$ with spatial decay rate α_H (see Appendix A) and field amplitude V_{-H}; the summation subscript H stands for all the TE and TM modes in this category.

III. The Plasma Fields

In the coupling region, near the waveguide openings in the perfectly conducting wall (see Figs. 2 and 3), at a given radian frequency ω, the plasma will be assumed to be described by its cold, inhomogeneous dielectric tensor. For simplicity, the inhomogeneity in the unperturbed density n_0 and applied magnetic field $\overline{B}_0 = \hat{z}B_0$ will be taken in the x-direction. The electromagnetic fields in the plasma can then be Fourier analyzed in y and z, and the complete solution for the fields, through Maxwell's equations, is determined by the solution of four coupled first-order, ordinary differential equations (o.d.e.'s) in x representing the coupling of "slow" and "fast" waves [6][7]. This is outlined in detail in Appendix B where the coupled o.d.e.'s are for the y and z Fourier analyzed tranverse (to x) fields $\overline{\mathcal{E}}_T(x, k_y, k_z)$ and $\overline{\mathcal{H}}_T(x, k_y, k_z)$, where $\overline{\mathcal{E}}_T = \hat{y}\mathcal{E}_y + \hat{z}\mathcal{E}_z$ and $\overline{\mathcal{H}}_T = \hat{y}\mathcal{H}_y + \hat{z}\mathcal{H}_z$. Without further approximations these equations must be solved numerically as follows. At the end of the coupling region into the plasma the "fast" and "slow"-wave fields will be assumed uncoupled and described by their WKB form. Furthermore, assuming that the plasma beyond the coupling region is absorptive, we can take the WKB form for each as outgoing waves of, say, unit amplitudes. The differential equations can then be integrated backwards in x to obtain $\overline{\mathcal{E}}_{T0} \equiv \overline{\mathcal{E}}_T(x = 0, k_y, k_z)$ and $\overline{\mathcal{H}}_{T0} \equiv \overline{\mathcal{H}}_T(x = 0, k_y, k_z)$ for all k_y and k_z of interest. The integration of the coupled differential equations for $\overline{\mathcal{E}}_T$ and $\overline{\mathcal{H}}_T$ must be carried out with care so that resonant (absorptive) or cutoff (evanescent) regions are properly taken into account for each pair of k_y and k_z. Further details of this are discussed in Section VI. The integration of the coupled differential equations can be considered to determine the matrix $\overline{\overline{Y}}(x)$ that gives

$$\overline{\mathcal{H}}_T(x) = \overline{\overline{Y}}_p(x) \cdot \overline{\mathcal{E}}_T(x) \tag{3}$$

where $\overline{\overline{Y}}_p = \overline{\overline{Y}}_p(x, k_y, k_z)$ is the plasma admittance matrix, defined in Appendix B (Eq. B13). The electromagnetic fields transverse to x in the plasma at $x = 0$ are then obtained by computing the inverse Fourier transform of $\overline{\mathcal{E}}_T(x = 0) \equiv \overline{\mathcal{E}}_{T0}$ and $\overline{\mathcal{H}}_T(x = 0) \equiv \overline{\mathcal{H}}_{T0}$

$$\overline{E}_T^P(x=0) = \int \frac{d^2k_T}{(2\pi)^2} \overline{\mathcal{E}}_{T0}\, e^{i\overline{k}_T \cdot \overline{r}_T} \tag{4}$$

$$\overline{H}_T^P(x=0) = \int \frac{d^2k_T}{(2\pi)^2} \overline{\mathcal{H}}_{T0}\, e^{i\overline{k}_T \cdot \overline{r}_T} \tag{5}$$

where $\overline{k}_T = \hat{y}k_y + \hat{z}k_z$ and $\overline{r}_T = \hat{y}y + \hat{z}z$, and using (3)

$$\overline{\mathcal{H}}_{T0} = \overline{\overline{Y}}_p(x=0)\cdot\overline{\mathcal{E}}_{T0} \equiv \overline{\overline{Y}}_{p0}\cdot\overline{\mathcal{E}}_{T0} \tag{6}$$

IV. The Waveguide-Plasma Coupling

For coupling with a single waveguide, as shown in Fig. 2, the waveguide transverse electric and magnetic fields at $x = 0$ must match onto the plasma fields, i.e.

$$\overline{E}_T^w(x=0) = \overline{E}_T^P(x=0) \tag{7}$$

and

$$\overline{H}_T^w(x=0) = \overline{H}_T^P(x=0)\,. \tag{8}$$

Using (1), (2), (4), (5), and (6) we can write (7) and (8) as

$$V_{+0}\,\bar{e}_d + \sum_H V_{-H}\,\bar{e}_H = \int \frac{d^2k_T}{(2\pi)^2}\overline{\mathcal{E}}_{T0}\,e^{i\bar{k}_T\cdot\bar{r}_T} \tag{9}$$

$$Y_d^w\frac{1-R}{1+R}\,V_{+0}\,\bar{h}_d - \sum_H Y_H^w V_{-H}\,\bar{h}_H = \int \frac{d^2k_T}{(2\pi)^2}\overline{\overline{Y}}_{p0}\cdot\overline{\mathcal{E}}_{T0}\,e^{i\bar{k}_T\cdot\bar{r}_T} \tag{10}$$

where we note that

$$Y_d^w\frac{1-R}{1+R} \equiv Y_d^{Pw} \tag{11}$$

is the admittance of the plasma presented to the dominant mode of the waveguide. Equations (9) and (10) determine, in principle, this admittance (and hence R) as well as the amplitudes of the higher-order modes per unit of incident field amplitude, i.e. $(V_{-H}/V_{+0}) \equiv \hat{V}_{-H}$. To write this out explicitly, we take the Fourier transform in y and z of (9) to obtain

$$\overline{\mathcal{E}}_{T0} = V_{+0}\,\bar{\epsilon}_d + \sum_H V_{-H}\,\bar{\epsilon}_H \tag{12}$$

where $\bar{\epsilon}_i = \int d^2r_T\, \bar{e}_i \exp(-i\bar{k}_T \cdot \bar{r}_T)$ is the Fourier transform of $\bar{e}_i$, and substitute (12) into (10) to find

$$Y_d^{Pw}\bar{h}_d - \sum_H Y_H^w \hat{V}_{-H}\bar{h}_H = \int \frac{d^2k_T}{(2\pi)^2}\overline{\overline{Y}}_{p0}\cdot\left[\bar{\epsilon}_d + \sum_H \hat{V}_{-H}\bar{\epsilon}_H\right]e^{i\bar{k}_T\cdot\bar{r}_T}. \tag{13}$$

Now, using the orthogonality properties of the waveguide field patterns (see Appendix A), and introducing the *coupling admittances*

$$Y_{ij} \equiv \int \frac{d^2k_T}{(2\pi)^2}\,\bar{\eta}_i^* \cdot \overline{\overline{Y}}_{p0}\cdot\bar{\epsilon}_j \tag{14}$$

where $\bar{\eta}_i = \int d^2r_T\,\bar{h}_i \exp(-i\bar{k}_T\cdot\bar{r}_T)$ in the Fourier transform of $\bar{h}_i$, we extract from (13)

$$Y_d^{Pw} - \sum_H Y_{dH}\hat{V}_{-H} = Y_{dd} \tag{15}$$

and

$$\sum_H (Y_{H'}^w\,\delta_{H'H} + Y_{H'H})\hat{V}_{-H} = -Y_{H'd}\,. \tag{16}$$

Equations (15) and (16) can be solved for the normalized higher-order mode field amplitudes $\hat{V}_{-H}$ and Y_d^{Pw} which by (12) determines the complex reflection coefficient R

$$R = \frac{1-\hat{Y}_d^{Pw}}{1+\hat{Y}_d^{Pw}}, \text{ where } \hat{Y}_d^{Pw} \equiv \frac{Y_d^{Pw}}{Y_d^w}\,. \tag{17}$$

Note that (15) represents the coupling of the dominant mode to the higher-order modes, and (16) gives the coupling of the higher-order modes among themselves.

The importance of higher-order modes can be determined by solving various truncated forms of (15) and (16). If we ignore all the higher-order modes, then from (15) we have simply

$$Y_d^{Pw} = Y_{dd} \tag{18}$$

If account is taken of one higher-order mode, say $H = 1$, (15) and (16) give a two-by-two matrix of equations which solves readily to give

$$Y_d^{Pw} = Y_{dd} - Y_{d1}\frac{Y_{1d}}{Y_1^w + Y_{11}} \tag{19}$$

and

$$\hat{V}_{-1} = \frac{-Y_{1d}}{Y_1^w + Y_{11}}\,. \tag{20}$$

In general (15) and (16) form a square matrix of equations of order equal to the number of higher-order modes plus one. For computational purposes proper ordering and truncation can be determined from estimates of (14) for different pairs of modes.

Having determined Y_d^{Pw} and the $\hat{V}_{-H}$, Eqs. (9) and (10) give

$$\bar{\mathcal{E}}_{T0} = V_{+0}\left[\bar{\epsilon}_d + \sum_H \hat{V}_{-H}\,\bar{\epsilon}_H\right] \tag{21}$$

$$\bar{\mathcal{H}}_{T0} = V_{+0}\left[Y_d^{Pw}\,\bar{\eta}_d - \sum_H Y_H^w\,\hat{V}_{-H}\,\bar{\eta}_H\right]. \tag{22}$$

Using (B12) and (B13) we can then obtain the electromagnetic field spectra in the plasma as excited by the dominant mode incident field amplitude (V_{+0}) in the waveguide, and the power flow into the plasma by Eqs. (B-14).

V. Coupling from Waveguide Arrays to the Plasma

In order to have more control on the excited spectrum of fields in the plasma it is common to use multiple wave-guides appropriately phased, i.e. waveguide arrays, as shown for example in Fig. 3. The coupling analysis of the preceding section is easily generalized to this case. The matching of the tangential $\overline{E}$ and $\overline{H}$ fields, (7) and (8), take on the more general form

$$\sum_w \left[V_{+0}^w\,\bar{e}_d^w + \sum_H V_{-H}^w\,\bar{e}_H^w\right] = \int \frac{d^2k_T}{(2\pi)^2}\,\bar{\mathcal{E}}_{T0}\,e^{i\bar{k}_T\cdot\bar{r}_T} \tag{23}$$

$$\sum_w \left[Y_d^{Pw}\,V_{+0}^w\,\bar{h}_d^w - \sum_H Y_H^w\,V_{-H}^w\,\bar{h}_H^w\right] = \int \frac{d^2k_T}{(2\pi)^2}\,\overline{\overline{Y}}_{P0}\cdot\bar{\mathcal{E}}_{T0}\,e^{i\bar{k}_T\cdot\bar{r}_T} \tag{24}$$

where the summation over the superscript w is over all the waveguides in the array. The Fourier transform of (23) gives

$$\bar{\mathcal{E}}_{T0} = \sum_w \left[V^w_{+0}\, \bar{\epsilon}^w_d + \sum_H V^w_{-H}\, \bar{\epsilon}^w_H \right] \tag{25}$$

where $\bar{\epsilon}^w_i(k_y, k_z) \leftrightarrow \bar{e}^w_i(y, z)$ is a Fourier transform pair, and using (25) in (24) we obtain

$$\sum_w \left[Y^{Pw}_d\, V^w_{+0}\, \bar{h}^w_d - \sum_H Y^w_H\, V^w_{-H}\, \bar{h}^w_H \right] = \int \frac{d^2k_T}{(2\pi)^2}\, \bar{\bar{Y}}_{p0} \cdot \sum_w \left[V^w_{+0}\, \bar{\epsilon}^w_d + \sum_H V^w_{-H}\, \bar{\epsilon}^w_H \right] e^{i\bar{k}_T \cdot \bar{r}_T} \tag{26}$$

Let the waveguides be designated by superscripts $w = \alpha, \beta, \gamma \ldots$, and the modes in each waveguide by the vertically aligned subscript $(i, j) = d$ or H. Using the orthogonality properties of the α-waveguide field patterns, and introducing the *coupling admittances*

$$Y^{\alpha w}_{ij} \equiv \int \frac{d^2k_T}{(2\pi)^2}\, \bar{\eta}^{\alpha *}_i \cdot \bar{\bar{Y}}_{p0} \cdot \bar{\epsilon}^w_j \tag{27}$$

where $\bar{\eta}^\alpha_i(k_y, k_z) \leftrightarrow \bar{h}^\alpha_i(y, z)$ is a Fourier transform pair, we find from (26)

$$Y^{P\alpha}_d - \sum_H Y^{\alpha\alpha}_{dH} \hat{V}^{\alpha\alpha}_{-H} - \sum_{\substack{w \neq \alpha \\ H}} Y^{\alpha w}_{dH}\, \hat{V}^{w\alpha}_{-H} = Y^{\alpha\alpha}_{dd} + \sum_{w \neq \alpha} Y^{\alpha w}_{dd}\, \hat{V}^{w\alpha}_{+0} \tag{28}$$

and

$$\sum_H (Y^\alpha_{H'}\, \delta_{H'H} + Y^{\alpha\alpha}_{H'H}) \hat{V}^{\alpha\alpha}_{-H} + \sum_{\substack{w \neq \alpha \\ H}} Y^{\alpha w}_{H'H}\, \hat{V}^{w\alpha}_{-H} = -Y^{\alpha\alpha}_{H'd} - \sum_{w \neq \alpha} Y^{\alpha w}_{H'd}\, \hat{V}^{w\alpha}_{+0} \tag{29}$$

where the mode amplitudes have been normalized to the incident dominant mode amplitude of waveguide α,

$$\hat{V}^{w\alpha}_{+0} \equiv \frac{V^w_{+0}}{V^\alpha_{+0}}; \quad \hat{V}^{\alpha\alpha}_{-H} \equiv \frac{V^\alpha_{-H}}{V^\alpha_{+0}}; \text{ and } \quad \hat{V}^{w\alpha}_{-H} \equiv \frac{V^w_{-H}}{V^\alpha_{+0}}. \tag{30}$$

The first two terms on the left-hand sides of (28) and (29) and the first terms on their right-hand sides are of course the same as in (15) and (16), respectively, and represent the coupling of all the

modes in waveguide α. The last term on the left-hand side of (28) represents the coupling of the dominant mode in waveguide α to the higher-order modes in all the other waveguides, and the last term on the left-hand side of (29) is due to the coupling of the higher-order modes in waveguide α to the higher-order modes in all the other waveguides. Finally, the second terms on the right-hand sides of (28) and (29) represent the driving by the incident dominant mode fields in all the other waveguides of, respectively, the dominant and higher-order modes in the α-waveguide. Note from (30) that the normalized, complex amplitudes $\hat{V}_{+0}^{w\alpha}$ contain the relative phasings in the incident dominant mode fields of the various waveguides.

Proceeding in a similar manner to apply to (26) the orthogonality properties of the field patterns of the other waveguides β, $\gamma, \ldots$ we obtain a set of equations (28) and (29) for each waveguide by simply replacing α with β, $\gamma, \ldots$. The simultaneous solution of all these sets of equations gives the higher-order mode amplitudes and reflection coefficient (through Y_d^{Pw} and (17)) in each of the waveguides. Again, proper ordering and truncation of all these equations can be arrived at from estimates of the coupling admittances (27). Thus using the results in (25) we can finally also find the electromagnetic field spectra in the plasma, (B12) and (B13), as excited by a given set of dominant mode incident field, complex amplitudes (V_{+0}^{w}) in the waveguide array, and the power flow into the plasma (B14).

VI. Summary and Discussion

We have derived a general formalism for the treatment of waveguide coupling in any frequency range, provided the slab geometry adopted for the plasma edge is valid. In particular, coupling in the ICRF and ECRF frequency ranges as well as LHRF can be treated by this method. Furthermore, the formalism accounts for finite waveguide dimensions both along and across $\overline{B}_o$, a feature neglected in all previous treatments of the problem, and allowance is made for the interaction of all possible waveguide modes.

The plasma is characterized by four coupled first-order differential equations which have to be solved for a complete spectrum of wavenumbers. In certain domains of wavenumber space, these equations can be uncoupled and solved analytically. This is illustrated in Appendix B. In general however, solutions must be found by numerical integration, and this was assumed in the text. We can proceed as follows. First, we specify a density profile which joins smoothly to a region of constant density far from the waveguides. In this region of constant density, plane

waves propagate, and by choosing only outgoing waves we satisfy the radiation conditions. Starting with arbitrary amplitudes, we integrate back to the waveguides at $x = 0$. This yields linear transfer matrices for $\overline{\mathcal{E}}_T(x)$ and $\overline{\mathcal{H}}_T(x)$ in terms of the amplitudes of the plane waves at large x. Eliminating these amplitudes yields the admittance matrix $\overline{\overline{Y}}_p(x)$ defined in Eq.(3), and with this admittance known, the problem is reduced to solving a set of linear equations in the waveguide mode amplitudes, as outlined in Sections IV and V, respectively, Eqs. 15 and 16 for a single waveguide and Eqs. 28 and 29 for multiple waveguides, i.e., waveguide arrays. In general the unknown waveguide mode amplitudes consist of the reflected wave of the dominant mode and all the higher-order modes. The coupling of these amplitudes in the linear equations, just mentioned, is given by Eqs. 14 and 27, respectively, for the single waveguide and the waveguide arrays.

We note that the backward, numerical integration of the plasma equations (B8–B11) assumes that the resonance $K_\perp \rightarrow 0$ does not occur in the coupling region. This is so in the LHRF where the LHR is chosen to be in the central part of the plasma. However, in the ICRF it may be that $K_\perp \rightarrow 0$ in the edge plasma region, indicating that coupling can occur to the slow-wave. In such cases Eqs. (B8–B12) may have to be supplemented with thermal correction terms.

Finally we would like to point out two limitations of the model and analysis presented. The first relates to the assumption that the plasma does not extend into the waveguides. Waveguides containing a plasma in a magnetic field can have very different mode structures [7] from empty waveguides and this may modify the linear coupling problem in an important way. Secondly, non-linear effects in the edge plasma, due to pondermotive forces [8], can modify the plasma dynamics and hence the coupling problem. Much attention has been given to this recently for coupling in the LHRF [9], [10], [11], [12].

Appendix A

In a uniform cylindrical waveguide with perfectly conducting walls of arbitrary cross section and free-space (ϵ_0, μ_0) medium the electromagnetic fields at a radian frequency $\omega = 2\pi f$ can be expressed by a superposition of an infinite set of orthogonal E (or TM) modes and H (or TE) modes. Together, these form a complete set and can represent an arbitrary electromagnetic field at a discontinuity in the waveguide. This representation of the fields is well-known and can be found in any standard text on electromagnetic fields, e.g. [5]. Here we summarize a convenient orthonormal form for these modes which we use in the text.

We take the direction of uniformity of the waveguide to be x and let all field quantities vary as $\exp(-i\omega t)$ where ω is taken as real. Each field quantity is expressed as the product of a function of x containing the propagation or evanescent properties and a function of $\bar{r}_T$, the two coordinates transverse to x, containing the mode functions that satisfy the boundary conditions on the particular cross section (C) of the waveguide. The transverse mode functions are found by solving the following Helmholtz equations with boundary conditions and normalization conditions:

E-modes	H-modes	
$\nabla_T^2\phi + p^2\phi = 0$	$\nabla_T^2\psi + p^2\psi = 0$	(A1)
$\phi = 0$ on C	$\hat{n}\cdot\nabla_T\psi = 0$ on C	(A2)
$p^2\int\lvert\phi\rvert^2 d^2r_T = 1$	$p^2\int\lvert\psi\rvert^2 d^2r_T = 1$	(A3)

Then

$\bar{e}_T = -\nabla_T\phi$	$\bar{h}_T = -\nabla_T\psi$	(A4)
$\bar{h}_T = \hat{x}\times\bar{e}_T$	$\bar{e}_T = -\hat{x}\times\bar{e}_T$	(A5)

are the transverse field pattern mode functions.

For each type of mode we obtain an infinite set of p-values and corresponding ϕ, ψ, $\bar{e}_T$ and $\bar{h}_T$ functions. The propagation functions in x for either type of mode are given by:

$$V(x) = V_+ e^{\gamma x} + V_- e^{-\gamma x} \tag{A6}$$
$$I(x) = Y^w(V_+ e^{\gamma x} - V_- e^{-\gamma x}) \tag{A7}$$

where

$$\gamma^2 = p^2 - k_0^2 \quad ; \quad k_0 = \frac{\omega}{c} \tag{A8}$$

$$\begin{aligned} &\text{for } k_0^2 > p^2 \quad , \quad \gamma \equiv ik \text{ (propagation)} \\ &\text{for } k_0^2 < p^2 \quad , \quad \gamma \equiv -\alpha \text{ (evanescence)} \end{aligned} \tag{A9}$$

and

$$Y^w = \begin{cases} (ik_0/\gamma)Y_0 & \text{for } E\text{-modes} \\ (\gamma/ik_0)Y_0 & \text{for } H\text{-modes} \end{cases} \tag{A10}$$

with $Y_0 \equiv \sqrt{\frac{\epsilon_0}{\mu_0}} \approx \frac{1}{120\pi \text{ Ohms}} \equiv \frac{1}{Z_0}$.

The complex electromagnetic fields can then be written as follows:

$$\bar{E}_T = \sum_n V_n(x)\, \bar{e}_n(\bar{r}_T) \tag{A11}$$

$$\bar{H}_T = \sum_n I_n(x)\, \bar{h}_n(\bar{r}_T) \tag{A12}$$

$$E_x = \sum_n \frac{ip_n^2}{k_0} Z_0\, I_n(x)\, \phi_n(\bar{r}_T) \tag{A13}$$

$$H_x = \sum_n \frac{ip_n^2}{k_0} Y_0\, V_n(x)\, \psi_n(\bar{r}_T)\,. \tag{A14}$$

In (A11) and (A12) n runs over all E-modes and H-modes; in (A13) n runs over only the E-modes; in (A14) n runs over only the H-modes.

The transverse field pattern mode functions satisfy the following orthogonality relations:

E-modes	H-modes	
$p_i^2 \int \phi_i \phi_j^{(*)} d^2 r_T = \delta_{ij}$	$p_i^2 \int \psi_i \psi_j^{(*)} d^2 r_T = \delta_{ij}$	(A15)
$\int \begin{Bmatrix} \bar{e}_i \cdot \bar{e}_j^{(*)} \\ \bar{h}_i \cdot \bar{h}_j^{(*)} \\ \bar{e}_i \times \bar{h}_j^{(*)} \end{Bmatrix} d^2 r_T = \delta_{ij}$	$\int \begin{Bmatrix} \bar{h}_i \cdot \bar{h}_j^{(*)} \\ \bar{e}_i \cdot \bar{e}_j^{(*)} \\ \bar{e}_i \times \bar{h}_j^{(*)} \end{Bmatrix} d^2 r_T = \delta_{ij}$	(A16)
$\int \bar{e}_i \cdot \bar{h}_j^{(*)} d^2 r_T = 0$	$\int \bar{e}_i \cdot \bar{h}_j^{(*)} d^2 r_T = 0$	(A17)

and among E-modes (sub e) and H-modes (sub h)

$$\int \begin{Bmatrix} \bar{e}_e \cdot \bar{e}_h^{(*)} \\ \bar{h}_e \cdot \bar{h}_h^{(*)} \\ \bar{e}_e \times \bar{h}_h^{(*)} \\ \bar{e}_h \times \bar{h}_e^{(*)} \end{Bmatrix} d^2 r_T = 0 \qquad (A18)$$

where the parenthesis around the star superscript on the function denotes that the equation holds with or without taking the complex conjugate of the function, and where δ_{ij} is the Kronecker function (i.e. equal to 1 for $i = j$, and equal to zero for $i \neq j$).

The time-averaged power flow in the waveguide is given by

$$P = \int \mathrm{Re}\left(\frac{1}{2}\bar{E}_T \times \bar{H}_T^*\right) \cdot \hat{x}\, d^2 r_T = \sum_m \frac{1}{2} Y_m^w \left(|V_{+m}|^2 - |V_{-m}|^2\right) \qquad (A19)$$

where the sum is only over those modes that are above cutoff, i.e. $k_0 > p_{rn}$.

For illustrative purposes, we also give the mode functions for the rectangular waveguide shown in Fig. 2:

E-modes

$$\phi_{mn} = C_{mn}^e \sin\frac{m\pi}{a} y \sin\frac{n\pi}{b} z \qquad (A20)$$

$$\left(p_{mn}^e\right)^2 = \left(\frac{m\pi}{a}\right)^2 + \left(\frac{n\pi}{b}\right)^2 \quad ; \quad \begin{matrix} m = 1, 2\ldots \\ n = 1, 2\ldots \end{matrix} \qquad (A21)$$

$$C^e_{mn} = \frac{2}{p^e_{mn}\sqrt{ab}} \tag{A22}$$

and

$\underline{H\text{-modes}}$

$$\psi_{mn} = C^h_{mn} \cos\frac{m\pi}{a}y \cos\frac{n\pi}{b}z \tag{A23}$$

$$\left(p^h_{mn}\right)^2 = \left(\frac{m\pi}{a}\right)^2 + \left(\frac{n\pi}{b}\right)^2 \quad ; \quad \begin{matrix} m = 0, 1, 2\ldots \\ n = 0, 1, 2\ldots \end{matrix} \quad m + n \neq 0 \tag{A24}$$

$$C^h_{mn} = \begin{cases} 2/p^h_{mn}\sqrt{ab} & \text{for } mn \neq 0 \\ \sqrt{2}/p^h_{mn}\sqrt{ab} & \text{for } mn = 0 \end{cases} \tag{A25}$$

Note that each mode requires two subscripts. Thus in (A11-14) the summing subscript must be taken to stand for a double subscript.

Note that the cutoff frequency of a mode is given by

$$f_c = \frac{p\,c}{2\pi} \tag{A26}$$

Thus, a mode is propagating if $f > f_c$, and then, by (A9), $\gamma = ik$ with

$$k = k_0\sqrt{1 - \left(\frac{f_c}{f}\right)^2}. \tag{A27}$$

On the other hand, a mode is evanescent if $f < f_c$ and then, by (A9), $\gamma \equiv -\alpha$ with

$$\alpha = p\sqrt{1 - \left(\frac{f_c}{f}\right)^2}. \tag{A28}$$

For $\underline{a > b}$, the dominant mode (i.e. the mode having the lowest cutoff frequency) is the H_{10} (i.e. TE_{10}) mode with $p^h_{10} = (\pi/a)$; if $b < (a/2)$, the next, higher-order mode is H_{20} with $p^h_{20} = (2\pi/a)$; on the other hand, if $b > (a/2)$ the next, higher-order mode would be H_{01} with $p^h_{01} = (\pi/b)$.

Appendix B

In this appendix we develop the electromagnetic field equations for an inhomogeneous, cold plasma in a magnetic field. The geometry is taken as shown in Figs. 2 and 3: the externally applied dc magnetic field $\overline{B}_0$ is in the z-direction, and the gradients in the unperturbed plasma density n_0 and in B_0 are both in the x-direction; the plasma is assumed homogeneous in the y and z directions.

We assume linear dynamics for the plasma particles and let the time dependence of all field quantities be $\exp(-i\omega t)$. Maxwell's equations for the electromagnetic fields in the plasma are then given by [7]

$$\nabla \times \overline{E} = i\omega\mu_0 \overline{H} \tag{B1}$$

$$\nabla \times \overline{H} = i\omega\epsilon_0 \overline{\overline{K}}(x,\omega) \cdot \overline{E} \tag{B2}$$

where

$$\overline{\overline{K}}(x,\omega) = \begin{pmatrix} K_\perp & -iK_\times & 0 \\ iK_\times & K_\perp & 0 \\ 0 & 0 & K_\parallel \end{pmatrix} \tag{B3}$$

with

$$K_\perp = (K_r + K_l)/2 \quad , K_\times = (K_r - K_l)/2 \tag{B4}$$

$$K_r(x,\omega) = 1 - \sum_s \frac{\omega_{ps}^2(x)}{\omega^2}\left(\frac{\omega}{\omega + p_s\Omega_s(x)}\right) \tag{B5}$$

$$K_l(x,\omega) = 1 - \sum_s \frac{\omega_{ps}^2(x)}{\omega^2}\left(\frac{\omega}{\omega - p_s\Omega_s(x)}\right) \tag{B6}$$

$$K_\parallel(x,\omega) = 1 - \sum_s \frac{\omega_{ps}^2(x)}{\omega^2} \tag{B7}$$

$\omega_{ps}^2 = (Z_s e)^2 n_{s0}(x)/m_s\epsilon_0$, $\Omega_s = Z_s eB_0(x)/m_s$, s designates the species of charged particle in the plasma, and p_s is the sign of the charge of particle s. In the above we have ignored collisions, but these can be easily included in properly modifying the above elements of $\overline{\overline{K}}$.

We normalize coordinate distances to (c/ω), e.g. $(\omega x/c) \equiv \xi$, and take the Fourier transform of the fields y and z: $\overline{\mathcal{E}}(\xi, n_y, n_z) \rightarrow \overline{E}$ *and* $\overline{\mathcal{H}}(\xi, n_y, n_z) \rightarrow \overline{H}$, where $n_y = (ck_y/\omega)$ *and* $n_z = (ck_z/\omega)$ are the indices of refraction in y and z, respectively, and k_y *and* k_z are the wavenumbers in these directions. Eliminating $\mathcal{E}_x$ and $\mathcal{H}_x$ from Maxwell's equations, Fourier-transformed in y and z, we find:

$$\frac{d\mathcal{E}_y}{d\xi} = -n_y \frac{K_\times}{K_\perp}\mathcal{E}_y + i\frac{n_y n_z}{K_\perp} Z_o \mathcal{H}_y + i\left(1 - \frac{n_y^2}{K_\perp}\right) Z_o \mathcal{H}_z \qquad (B8)$$

$$\frac{d\mathcal{E}_z}{d\xi} = -n_z \frac{K_\times}{K_\perp}\mathcal{E}_y - i\left(1 - \frac{n_z^2}{K_\perp}\right) Z_o \mathcal{H}_y - i\frac{n_y n_z}{K_\perp} Z_o \mathcal{H}_z \qquad (B9)$$

$$\frac{dZ_o\mathcal{H}_y}{d\xi} = -in_y n_z \mathcal{E}_y + i(n_y^2 - K_\parallel)\mathcal{E}_z \qquad (B10)$$

$$\frac{dZ_o\mathcal{H}_z}{d\xi} = -i\left(n_z^2 - K_\perp + \frac{K_\times^2}{K_\perp}\right)\mathcal{E}_y + in_y n_z \mathcal{E}_z - \frac{K_\times}{K_\perp} n_z\, Z_o \mathcal{H}_y + \frac{K_\times}{K_\perp} n_y\, Z_o \mathcal{H}_z \qquad (B11)$$

In all of the above equations $K_\perp$, $K_\times$ and $K_\parallel$ are functions of ξ,and $Z_o = \sqrt{\mu_0/\epsilon_o}$. These equations are all first order and are well suited for a numerical treatment. The only singularity in the coefficients occurs when $K_\perp \rightarrow 0$, which is simply the hybrid resonance (lower or upper hybrid). If we impose the values of $\mathcal{E}_y$ and $\mathcal{E}_z$ at $x = 0$, and require that only outgoing or evanescent waves exist as $x \rightarrow \infty$, then these boundary conditions determine completely the solution of Eqs.(B8–B11). We thus obtain

$$\overline{\mathcal{E}}_T(x) = \overline{\overline{S}}(x) \cdot \overline{\mathcal{E}}_T(x = 0) \qquad (B12)$$

In particular,$\mathcal{H}_y(x)$ and $\mathcal{H}_z(x)$ are linear functions of $\mathcal{E}_y(x)$ and $\mathcal{E}_z(x)$, and this can be expressed by the plasma admittance matrix $\overline{\overline{Y}}_P(x)$:

$$\overline{\mathcal{H}}_T(x) = \overline{\overline{Y}}_p(x) \cdot \overline{\mathcal{E}}_T(x) \qquad (B13)$$

The plasma admittance matrix $\overline{\overline{Y}}_{po} = \overline{\overline{Y}}_p(x = 0)$, which enters into all the coupling admittances (Eqs. 14 and 27), can be determined numerically as outlined in Section II. Finally, the time-averaged power flow in x, into the plasma, is given by

$$P_p = \int_{-\infty}^{\infty} dy \int_{-\infty}^{\infty} dz\, Re\frac{1}{2}\left(\overline{E}_T \times \overline{H}_T\right)\cdot\hat{x}$$

$$= \int_{-\infty}^{\infty} \frac{dk_y}{2\pi} \int_{-\infty}^{\infty} \frac{dk_z}{2\pi}\, Re\frac{1}{2}\left(\overline{\mathcal{E}}_T \times \overline{\mathcal{H}}_T\right)\cdot\hat{x} \qquad (B14)$$

where the last expression is obtained by using Parseval's theorem.

In the rest of this Appendix we consider regimes where Eqs.(B8–B11) can be treated analytically. Simplified and familiar equations can be obtained if we set $K'_\perp = 0 = K'_\times$ where the prime denotes the derivative with respect to ξ (but retain $K_\parallel$, $K_\perp$, and $K_\times$ as functions of ξ), and $n_y = 0$. Eliminating $\mathcal{H}_y$ and $\mathcal{H}_z$ we then find:

$$\mathcal{E}''_y + \left(\frac{K_\times^2}{n_z^2 - K_\perp} + K_\perp - n_z^2\right)\mathcal{E}_y = -\left(\frac{n_z K_\times}{n_z^2 - K_\perp}\right)\mathcal{E}'_z \qquad (B15)$$

$$\mathcal{E}''_z - \frac{K_\parallel}{K_\perp}(n_z^2 - K_\perp)\mathcal{E}_z = -\frac{n_z K_\times}{K_\perp}\mathcal{E}'_y \qquad (B16)$$

In the LHRF (lower-hybrid range of frequencies), $K_\parallel \gg 1$ near the plasma edge and (B15–B16) are essentially uncoupled, the first giving the "fast wave" equation ($\mathcal{E}_z \simeq 0$) and the second one giving the "slow wave" equation ($\mathcal{E}_y \simeq 0$). In the ICRF (ion-cyclotron range of frequencies) $\mathcal{E}_z \approx 0$ and $\mathcal{E}'_z \approx 0$, and (B15) then gives the "fast wave" equation. Thus the uncoupled equations (B15and B16) have been solved for slow-wave coupling in LHRF [1], fast-wave coupling in LHRF [4], and fast-wave coupling in ICRF [13]. In the ECRF regime, Eqs.(B15-B16) do not uncouple as simply because near the edge fast and slow waves have comparable perpendicular wave numbers (since $K_\parallel \simeq K_{\perp,\times}$). Thus when $\omega \simeq \Omega_e$ the full fourth order system has to be solved.

For $n_y \neq 0$ an approximate decoupling can be obtained in the LHRF, at least in most regions of n_y, n_z space. As a first approximation, we set $K'_\perp \simeq 0$, where the prime denotes a spatial derivative. For the fast–wave we set $\mathcal{E}_z = 0$. It can be shown that the correction is roughly $\mathcal{E}_z \approx |K_\times^2/K_\parallel|\mathcal{E}_y \ll \mathcal{E}_y$; thus, letting $\mathcal{E}_y \equiv \mathcal{E}_F$, we find approximately near the plasma edge

$$\mathcal{E}''_F + \left[\frac{K_\times^2}{n_z^2 - K_\perp} + K_\perp - n_y^2 - n_z^2 + \frac{n_y K'_\times}{n_z^2 - K_\perp}\right]\mathcal{E}_F = 0 \qquad (B17)$$

and hence the fast–wave field components:

$$\mathcal{E}_y^{(F)} \approx \mathcal{E}_F \tag{B18}$$
$$\mathcal{E}_z^{(F)} \approx 0 \tag{B19}$$

For the slow–wave, noting that for $K_\times^2 \ll (-K_\parallel)$, it is found from Eqs.(B8–B11) that for the largest terms to balance, we need $\mathcal{E}_y \approx [n_y n_z/(n_z^2 - K_\perp)]\mathcal{E}_z$; letting $\mathcal{E}_z \equiv \mathcal{E}_S$, we find approximately

$$\mathcal{E}_S'' + \left[-\frac{K_\parallel}{K_\perp}(n_z^2 - K_\perp) - n_y^2\right]\mathcal{E}_S = 0 \tag{B20}$$

and the approximate slow–wave field components are:

$$\mathcal{E}_y^{(s)} \approx \frac{n_y n_z}{n_z^2 - K_\perp}\mathcal{E}_S \tag{B21}$$
$$\mathcal{E}_z^{(s)} \approx \mathcal{E}_S \tag{B22}$$

The analytical solutions of (B17, B20) are straightforward. We assume LHRF parameters, and take $K_\perp \simeq 1, K_\parallel = \alpha x$ and $K_\times = \beta x$ in the coupling region, where $\alpha \gg 1$. We find the solutions:

$$\mathcal{E}_F(x) = \frac{\mathrm{U}(a, 2\beta^{1/2}x/(1-n_z^2)^{1/4})}{\mathrm{U(a,0)}} \tag{B23}$$
$$\mathcal{E}_S(x) = \frac{\mathrm{Ai}(e^{-i\pi/3}\alpha^{1/3}(n_z^2-1)^{1/3}\,x)}{\mathrm{Ai}(0)} \tag{B24}$$

where $\mathcal{E}_{F,S}(0) \equiv 1$ and where U and Ai are the parabolic cylinder and Airy function respectively[14]. Branch cuts are so defined that for $|n_z| < 1$ we have $(1-n_z^2)^{1/4} = |1-n_z^2|^{1/4}$, $(n_z^2-1)^{1/3} = e^{i\pi/3}|1-n_z^2|^{1/3}$ and for $|n_z| > 1$ we have $(1-n_z^2)^{1/4} = e^{i\pi/4}|n_z^2-1|^{1/4}$, $(n_z^2-1)^{1/3} = e^{i2\pi/3}|n_z^2-1|^{1/3}$. We have also defined:

$$a = -\frac{(1-n_z^2)^{1/2}}{2\beta}\left(\frac{\beta n_y}{1-n_z^2} + (1-n_z^2-n_y^2)\right) \tag{B25}$$

Eqs.(B17,B20) are valid provided we assume fast and slow waves satisfy uncoupled differential equations. Careful inspection of the system (B8-B11) shows that the uncoupling assumption breaks

down when either $n_z^2 \to 1$ or when $n_y^2 + n_z^2 \to 1$. In the first case, the confluence of slow and fast waves, as indicated by the local dispersion relation, occurs very close to the edge, and it is not surprising that the corresponding differential equations become strongly coupled. In the second case, the free-space wavelength at the edge becomes infinite as $n_y^2 + n_z^2 \to 1$, and decoupling the equations by arguing that one wave is much shorter than the other is not valid.

To use the approximate equations (B17, B20), we find the magnetic fields from Faraday's law in terms of $\mathcal{E}_y$ and $\mathcal{E}_z$. We find

$$\overline{\mathcal{H}}_T = \overline{\overline{Y}}_{TT} \cdot \overline{\mathcal{E}}_T + \overline{\overline{Y}}_{TT'} \cdot \frac{d}{d\xi} \overline{\mathcal{E}}_T \tag{B26}$$

where

$$\overline{\overline{Y}}_{TT} = Y_0 \begin{pmatrix} \dfrac{in_z K_\times}{n_{yz}^2 - K_\perp} & 0 \\ \dfrac{-in_y K_\times}{n_{yz}^2 - K_\perp} & 0 \end{pmatrix} \tag{B27}$$

and

$$\overline{\overline{Y}}_{TT'} = Y_0 \begin{pmatrix} \dfrac{-in_y n_z}{n_{yz}^2 - K_\perp} & i\dfrac{n_y^2 - K_\perp}{n_{yz}^2 - K_\perp} \\ -i\dfrac{n_z^2 - K_\perp}{n_{yz}^2 - K_\perp} & \dfrac{in_y n_z}{n_{yz}^2 - K_\perp} \end{pmatrix} \tag{B28}$$

where we have written $n_y^2 + n_z^2 \equiv n_{yz}^2$. For Eqs.(B17, B20) we then have:

$$\overline{\overline{Y}}_{p0}(n_y, n_z) = Y_0 \begin{pmatrix} 0 & \dfrac{i}{n_z^2 - 1} \\ 0 & 0 \end{pmatrix} \mathcal{E}_S'(0) +$$

$$+ Y_0 \frac{i}{n_{yz}^2 - 1} \begin{pmatrix} -n_y n_z & \dfrac{n_y^2 n_z^2}{n_z^2 - 1} \\ -(n_z^2 - 1) & n_y n_z \end{pmatrix} \mathcal{E}_P'(0) \tag{B29}$$

where:

$$\mathcal{E}'_S(0) = \alpha^{1/3} e^{-i\frac{\pi}{3}} (n_z^2 - 1)^{1/3} \frac{\mathrm{Ai}'(0)}{\mathrm{Ai}(0)} \qquad (B30)$$

$$\mathcal{E}'_F(0) = -\frac{2\beta^{1/2}}{(1-n_z^2)^{1/4}} \frac{\Gamma(\frac{3}{4}+\frac{a}{2})}{\Gamma(\frac{1}{4}+\frac{a}{2})} \qquad (B31)$$

where "α" is given in Eq.(B25). This expression for $\overline{\overline{Y}}_{p0}(n_y, n_z)$ can then be used in the integral of Eq.(14) or (27). A problem arises however with the resonant denominators in the second term of Eq.(B29), because some of the singularities are not integrable. This is because, as noted above, Eqs.(B17and B20) break down when $|n_z| \to 1$ or when $|n_{yz}| \to 1$. In fact the resonant denominators in $\overline{\overline{Y}}_{P0}$ should disappear when the full sytem of equations is treated correctly in the limit $|n_z|, |n_{yz}| \to 1$. Presumably this can only be done by numerical means. Thus Eq.(B17,B20,B29) are useful only if the excitation spectrum has little energy near these resonances. In this case, the singularities in the integration of Eqs.(14) or (27) can be avoided by arbitrarily setting the spectrum to zero near these resonances.

For the ICRF the interest has been to couple to the fast wave. The simplest analysis has set $n_y = 0, K'_\perp = 0, K'_\times = 0$, and ignored coupling to the slow-wave by assuming $\mathcal{E}_z = \mathcal{E}'_z = 0$, *ab initio* [13]; this then results in Eq.(B15) with the right hand side equal to zero, which can be readily solved. Recently, the effects of nonzero n_y have been shown to require the study of a more complex equation which follows from Eqs.(B8–B11) by retaining $K'_\perp$ and $K'_\times$ while still assuming $\mathcal{E}_z = \mathcal{E}'_z = 0$ [15]:

$$\frac{d^2\mathcal{E}_y}{d\xi^2} + f(\xi)\frac{d\mathcal{E}_y}{d\xi} + g(\xi)\mathcal{E}_y = 0 \qquad (B32)$$

where:

$$f(\xi) = \frac{n_y^2 K'_\perp}{(K_\perp - n_z^2)(K_\perp - n_y^2 - n_z^2)} \qquad (B33)$$

$$g(\xi) = K_\perp - n_y^2 - n_z^2 - \frac{K_\times}{K_\perp - n_z^2} + n_y \frac{K'_\times}{K_\perp - n_z^2} - \frac{n_y K_\times K'_\perp}{(K_\perp - n_z^2)(K_\perp - n_y^2 - n_z^2)} \qquad (B34)$$

The assumption of neglecting the coupling to the slow wave can be partially justified by assuming that at the exciting structure the plasma density is finite so that $K_\parallel$ is sufficiently large to short-out

the $\mathcal{E}_z$ field, and $K_\perp \neq 0$. To gauge the importance of nonzero n_y, calculations have been carried-out (for current sheets rather than waveguides) on a simplified equation that retains $K_\perp(\xi)$ and $K_\times(\xi)$ but sets $K'_\perp = K'_\times = 0$ [16]. This is just Eq.(B15) with the right-hand side set equal to zero and the second term supplemented by n_y^2. More recent calculations show however that this local approximation is not always valid[17]. Finally, we remark that great interest attaches also to the possibility of coupling with a waveguide to the slow-wave in the ICRF[18]. This of course can also be treated by the formalism developed in this paper.

REFERENCES

[1] BRAMBILLA, M., Nucl. Fusion **16** (1976) 47.

[2] KRAPCHEV, V., BERS, A., Nucl. Fusion **18** (1978) 519.

[3] BRAMBILLA, M., Nucl. Fusion **19** (1979) 1343.

[4] THEILHABER, K., BERS, A., Nucl. Fusion **20** (1980) 547.

[5] MARCUVITZ, N., *Waveguide Handbook*, M.I.T. Radiation Laboratory Sciences, Vol. 10, McGraw-Hill Book Co.,Inc., New York, 1951. COLLIN, R.E., *Field Theory of Guided Waves*, McGraw-Hill Book Co.,Inc., New York, 1960. HARRINGTON, R. F., *Time Harmonic Electromagnetic Fields*, McGraw-Hill Book Co. Inc., New York 1961.

[6] In a local sense, the solution of the fourth-order dispersion relation for a cold plasma, with given ω, k_y *and* k_z, results in two values of k_x^2 [7]; we call the larger one the "slow" wave and the smaller one the "fast" wave.

[7] ALLIS,W. P., BUCHSBAUM, S.J., BERS, A., *Waves in Anisotropic Plasmas*, MIT Press, Cambridge, Mass. 1963.

[8] KRAPCHEV, V., BERS, A., *Third Topical Conf. on RF Plasma Heating, California Institute of Technology*, Pasadena, California, Jan 11–13, 1978, pp. G5.1–G5.4.

[9] CHAN, V., CHIU, S., *Phys. Fluids*, **20**, 1977, 1164.

[10] FUKUYAMA, A., MORISHITA, T., FURUTANI,Y., *Plasma Phys.* **22**, 1980, 565.

[11] KRAPCHEV, V., THEILHABER, K., KO, K., BERS, A., *Phys. Rev. Lett.*, **46**, 1981, 1398.

[12] THEILHABER, K., *Nonlinear Coupling to Lower Hybrid Waves in a Tokamak Plasma*, Doctoral Thesis, Massachusetts Institute of Technology, Cambridge, Massachusetts, also report PFC/JA–81–18, Plasma Fusion Center, M.I.T., September 1981.

[13] ADAM, J., Report EUR-CEA-FC-1004, Association Euratom-CEA,Fontenay–aux–Roses,France,1979.

[14] ABRAMOWITZ, M., STEGUN, I. A., *Handbook of Mathematical Functions*, National Bureau of Standards, Tenth Printing,1970, pp. 435, 685.

[15] BERS, A., JACQUINOT, J., LISTER, G., 2^{nd} Joint Varenna-Grenoble Int. Symposium, Como: Report EUR-CEA-FC-1066, Association Euratom-CEA, Fontenay–aux–Roses, France, September 1980.

[16] BERS, A., HARTEN, L. P., RAM, A., Proceedings Fourth Topical Conf. on RF Heating in

Plasma, February 9-10, 1981, University of Texas, Austin Texas, pp. A.16–A.20.

[17] RAM, A., BERS, A., HARTEN, L., *to be published.*

[18] ONO, M., WONG, K-L., Phys. Rev. Letters, 45 (1980) 1105.

Acknowledgements

This work was supported in part by the US–DOE Contract DE–AC 02–78–ET–51013, and in part by the US–NSF Grant No. ENG 79–07047. We also wish to thank J. Freidberg and D. Hewitt for several useful discussions.

Figure Captions

Figure 1

Waveguide–plasma coupling geometry. The coupling region extends from the plasma wall into the edge plasma; it does not include the hot, central plasma where the excited waves are assumed to be dissipated. For a large plasma the coupling region can be modeled in slab geometry.

Figure 2

Geometry used in the analysis of coupling from a single waveguide to a plasma.

Figure 3

Geometry used in the analysis of coupling from multiple waveguides – waveguide arrays – to a plasma.

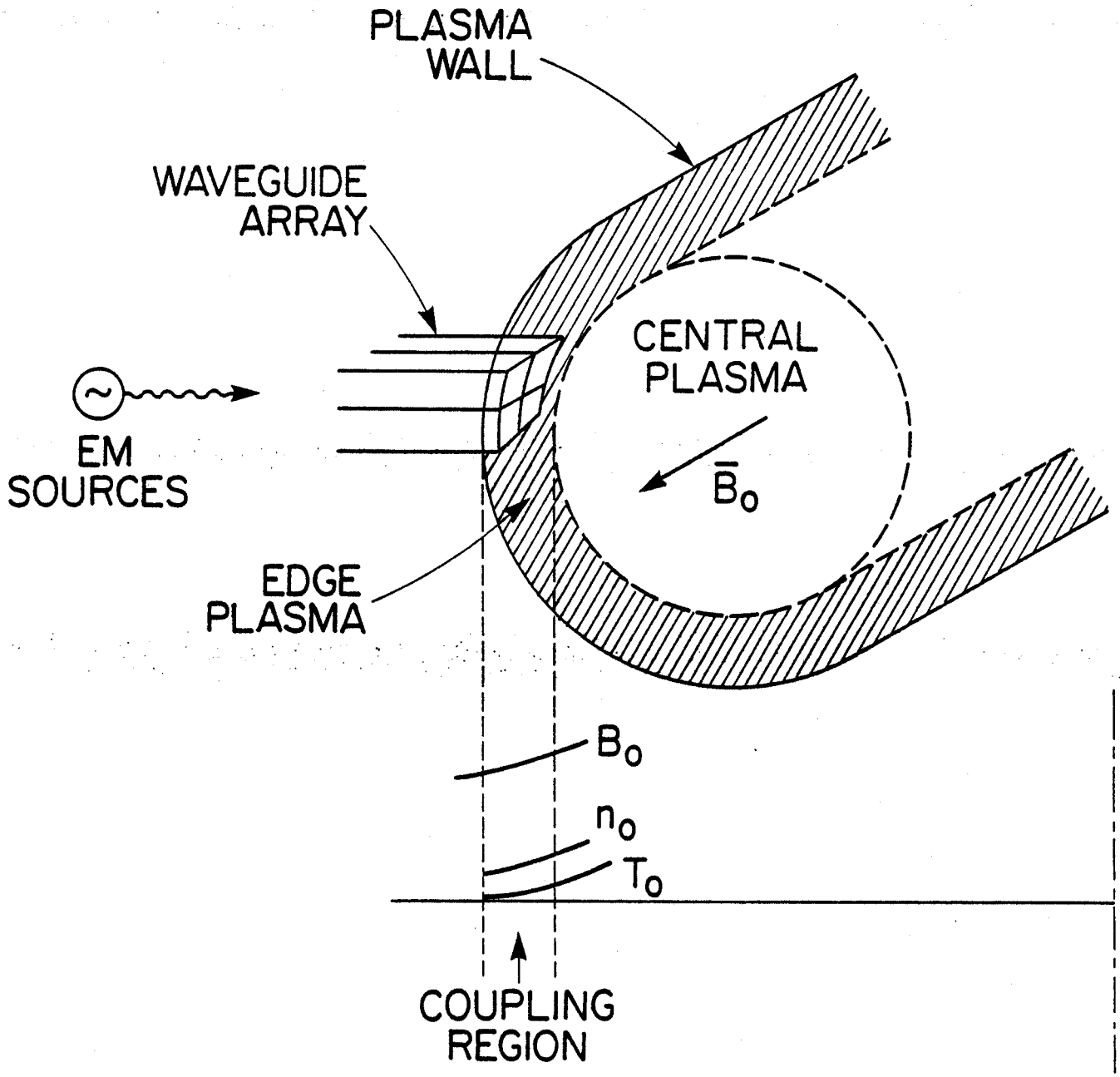
PLASMA
WALL
WAVEGUIDE
ARRAY
CENTRAL
PLASMA
$\bar{B}_o$
EM
SOURCES
EDGE
PLASMA
B_o
n_o
T_o
COUPLING
REGION

FIGURE 1

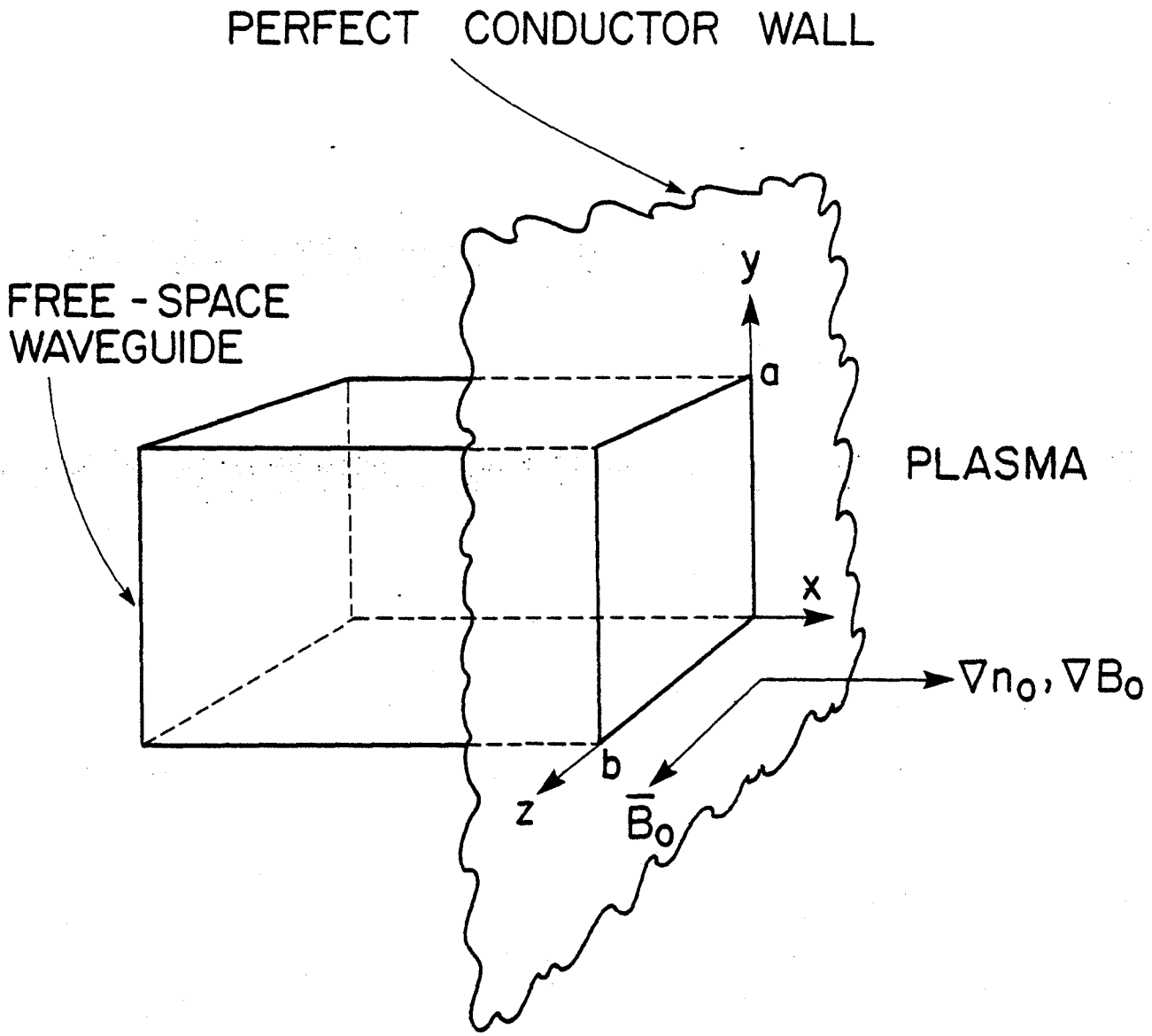
PERFECT CONDUCTOR WALL
FREE - SPACE WAVEGUIDE
y
a
PLASMA
x
$\nabla n_o, \nabla B_o$
b
z
$\bar{B}_o$

FIGURE 2

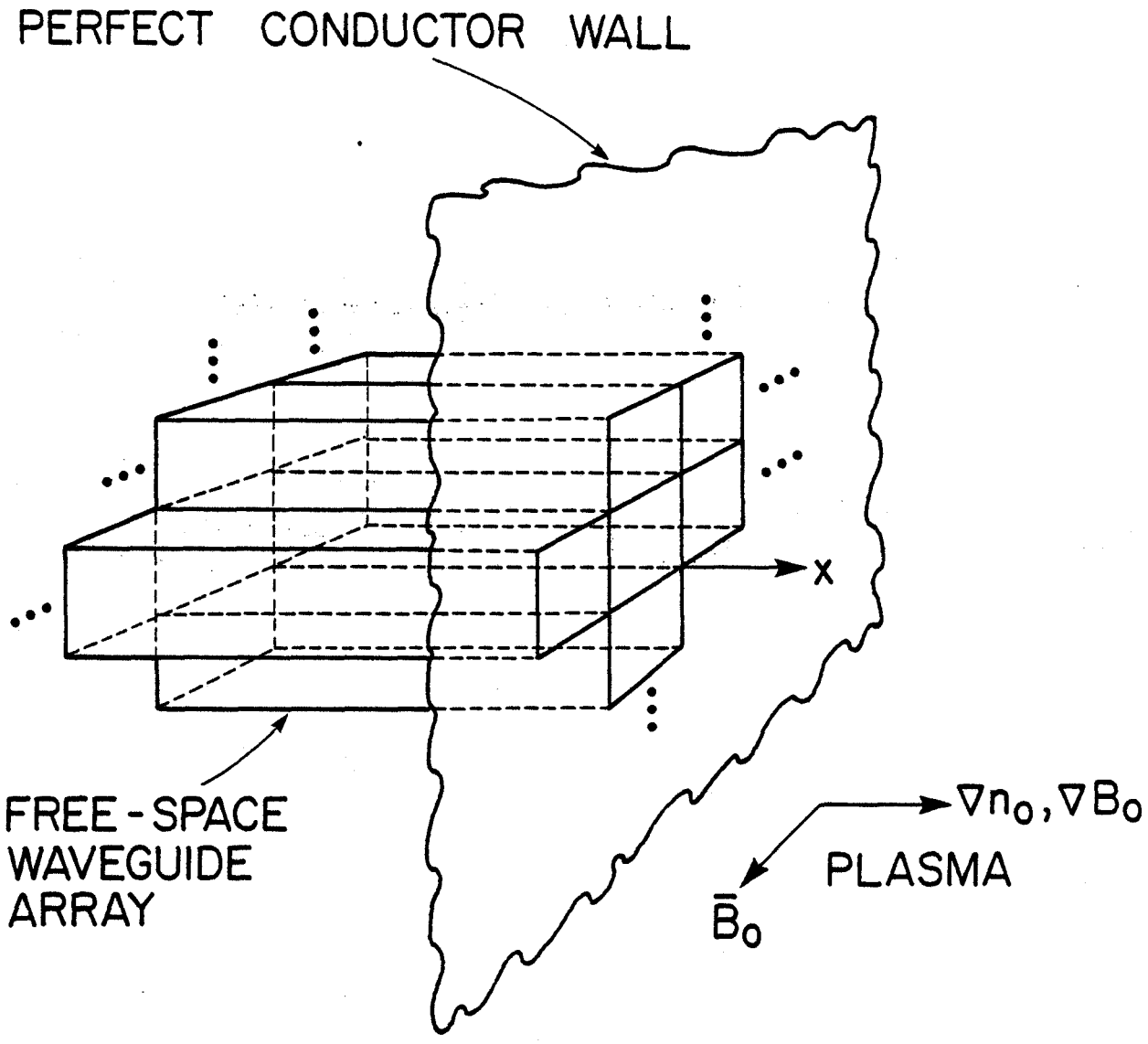
PERFECT CONDUCTOR WALL
x
FREE-SPACE
WAVEGUIDE
ARRAY
$\nabla n_0, \nabla B_0$
PLASMA
$\bar{B}_0$

FIGURE 3